Applied Catalysis B: Environmental 96 (2010) 67–71

Contents lists available at ScienceDirect

Applied Catalysis B: Environmental

journal homepage: www.elsevier.com/locate/apcatb

New materials for photocatalytic degradation of Indigo Carmine—Synthesis, characterization and catalytic experiments of nanometric tin dioxide-based composites

M.G. Coelho [a], G.M. de Lima [a,*], R. Augusti [a], D.A. Maria [b], J.D. Ardisson [b]

[a] Departamento de Química, UFMG, Av. Antonio Carlos 6627, CEP 31270-901, Belo Horizonte, MG, Brazil
[b] Laboratório de Física Aplicada – CDTN/CNEN, Belo Horizonte, MG, Brazil

ARTICLE INFO

Article history:
Received 18 June 2009
Received in revised form 27 January 2010
Accepted 1 February 2010
Available online 6 February 2010

Keywords:
Pyrolysis
Organotin derivatives
Tin oxide
Photocatalysis
Environment contaminants

ABSTRACT

Herein we describe experiments of photocatalytic degradation of Indigo Carmine dye, carried out by new composites containing nanometric SnO_2 supported on Al_2O_3. The composites were prepared in a sequence of procedures which involved reactions of $SnBuCl_3$, aluminium hydroxide with NH_4OH in ethanol in order to impregnate organotin oxide in Al_2O_3 in different stoichiometry. Hence, the obtained materials were employed in experiments of thermal decomposition in O_2 at different temperatures, yielding nanoparticles of SnO_2 supported on Al_2O_3, with ratios of Sn/Al_2O_3 of 30% (**1**), 40% (**2**) and 60% (**3**) in weight, respectively. XRD experiments revealed diffraction patterns of SnO_2, and those of Al_2O_3 were not observed due to their low crystallinity. ^{119}Sn Mössbauer experiments suggested the formation of SnO_2 in all experiments. Studies of scanning electron microscopies (SEM) showed the formation of tin(IV) oxide on the surface of Al_2O_3 in composites (**1**)–(**3**). The crystallite average size (D) was calculated employing Scherrer equation, revealing the presence of nanometric SnO_2 in all samples. Photocatalytic degradation of Indigo Carmine in aqueous medium, induced by composites (**1**)–(**3**), was monitored by electronic spectroscopy, and composite (**3**) displayed the higher activity. In addition, results from electrospray ionization mass spectrometry (ESI-MS) and tandem mass spectrometry (ESI-MS/MS) allowed us to propose a degradation route for the dye.

1. Introduction

Tin(IV) oxide, SnO_2 (rutile type structure) is a well established n-type semiconductor with a wide band gap (E_{gap} = 3.6 eV at 300 K), which due to its (i) high thermal stability in air (>500 °C), (ii) low cost and (iii) ability to aggregate dopants to enhance sensitivity or selectivity, has been employed in many catalytic processes [1–4]. Synthetic methods such as CVD [5–7], electrodeposition [8,9] electron beam evaporation [10], pyrolysis [11], sputtering of Sn targets [12,13], hydrothermal synthesis [14], reactions in liquid ammonia [15], pulsed laser deposition [16], mechano-chemical [17] and sol gel precipitation [18] have been used [19]. Our group, for example, has employed the thermal decomposition of organotin oxides to prepare nanosized particles of SnO_2 [20]. On this matter we have found that the choice of a particular organotin precursor is of some importance [21–27].

A most significant application of SnO_2 is as gas sensors [28]. Among the many other reported reactions using SnO_2 as catalyst [29] are conversions of alcohols or aldehydes to ketones [30], simultaneous reductions of SO_2 and NO, and reduction of RSSR, when supported on TiO_2 [31]. In addition, SnO_2 has potential in methane and methanol reforming processes [32]. Another useful application is in the conversion of soybean oil into biodiesel, with yields up to 93% [33,34].

The photocatalytic potential of SnO_2-based composites in the removal of methylene blue (MB) pollutants [35] has been reported. These results encouraged us to further investigate the SnO_2/Al_2O_3 in the degradation of Indigo Carmine. This pigment has been used for many years in industries, such as textile, paper, and plastics, and as colorant. Even in very small quantity dyes can be easily recognized either in industrial products or in the wastewaters [36–38]. Stability, an important property of dyes, prevents treatment of their aqueous residues, even when it is present in low concentrations. Commonly used methods are either economically unfavorable and/or technically complicated [39].

Degradation of dyes in aqueous solution has been studied using TiO_2 immobilized on the inner surfaces of quartz pipes with continuous exposure to UV light [40]. It has been shown [41] on a small scale that TiO_2 plus solar irradiation is an efficient system for color removal from aqueous solutions containing Indigo Carmine.

* Corresponding author.
E-mail addresses: gmlima@ufmg.br, delima.geraldo@gmail.com (G.M. de Lima).

0926-3373/$ – see front matter © 2010 Elsevier B.V. All rights reserved.
doi:10.1016/j.apcatb.2010.02.002

Other articles have reported that treatment with hydrogen peroxide and transition metal complexes effected not only color removal but also almost complete mineralization of the dye [42].

Here we describe the preparation and characterisation of nanometric SnO_2 supported on Al_2O_3 and results of the photocatalytic degradation of Indigo Carmine.

2. Experimental

2.1. Chemicals

Indigo Carmine and organotin halides were purchased from Sigma–Aldrich (Milwaukee, WI) and used without further purification. Doubly distilled water was used to prepare solutions.

2.2. Instrumentation and techniques

Thermal preparation of the supported material was carried out in a tube furnace in O_2 to atmosphere using a flux of 100 mL min^{-1} at temperatures of 430 °C for (**1**) and (**2**), and 600 °C for sample (**3**).

XRD patterns were collected with a Siemens D5000 instrument using a Ni-filtered Cu K_α radiation (λ = 1.5418 Å) and a graphite monochromator in the diffracted beam. A scan rate of 1°/min was applied to record a pattern in the 2θ range of 20–80°. Silicon was used as internal standard. The XRD lines encountered in JCPDS (Joint Committee on Powder Diffraction Standards) [43] of Al_2O_3 (card 46-1212) and SnO_2 (card 41-1445) were used as standard.

^{119}Sn Mössbauer measurements were performed on a conventional apparatus with the samples at liquid N_2 temperature, using a $CaSnO_3$ as source of γ radiation, kept at room temperature.

Scanning electron microscopic images (SEM) were taken using a JEOL JSM-840A instrument with samples covered with a thin layer of gold. The X-ray electron probe microanalyses (EPMA) were carried out using a JXA 89000 RL wavelength/energy dispersive combined microanalyser with samples covered with a thin film of carbon deposited by sputtering.

UV–vis measurements were performed by using a Hitachi U-2010 spectrophotometer.

ESI-MS and ESI-MS/MS analyses were performed with a LCQ Fleet mass spectrometer (ThermoScientific, San Jose, CA) operating in the negative ion mode. The reaction aliquots were directly infused into the ion source at a flow rate of 20 μL min^{-1} using a microsyringe (Hamilton Company, Reno, NV) and the mass spectra obtained as an average of 50 scans, each one requiring 0.2 s. Typical ESI conditions were as follows: heated capillary temperature 300 °C; sheath gas (N_2) flow rate 20 units (ca. 0.3 L min^{-1}); spray voltage 4 kV; capillary voltage 25 V; tube lens offset voltage 25 V. For the ESI-MS/MS experiments, the precursor ions were first isolated within the ion trap and fragmented upon collision with helium. Collision energies were adjusted to yield detectable product ions.

2.3. Preparation of the supported material

A solution of $SnBuCl_3$ and NH_4OH was successively added to a suspension of $Al(OH)_3$ in EtOH. After 90 min of reflux, the reaction mixture was filtered and the white precipitate was washed with hot water in order to remove non-reacted inorganic materials. Following further washing with ethanol and ethyl ether, the material was dried overnight in a vacuum desiccator charged with silica gel. Samples of Sn/Al_2O_3 were prepared to have after pyrolysis and amount of Sn of 30% (**1**), 40% (**2**) and 60% (**3**) in weight. The dry samples were decomposed in a tube furnace in O_2 atmosphere at temperatures of 430 °C for (**1**) and (**2**), and 600 °C for sample (**3**).

2.4. Experiments of photocatalysis

The material (**1**), (**2**), (**3**) or SnO_2 (30 mg), was added to an aqueous solution of Indigo Carmine (100 mL; 30 μmol L^{-1}) and the pH adjusted to 5, using H_2SO_4 (M = 0.1 mol L^{-1}). The reaction mixture was exposed to ultraviolet (UV) irradiation (UV lamp: Philips HPL–N 30 W). Aliquots were taken at intervals of 20 min, filtered using a 0.45 μm filter (Millipore, Jaffrey, NH) to eliminate solid particles and kept protected from light in a refrigerator prior to ESI-MS and UV–vis analysis.

2.5. Calibration curve

Several aqueous solutions of Indigo Carmine were prepared at assorted concentrations (30, 20, 10, 7.5, 6 and 3 μmol L^{-1}) and their absorbance measured at 610 nm (λ_{max} of the dye). The resulting plot (not shown) displayed an excellent linear relationship with R^2 = 0.999.

3. Results and discussion

As stated in Section 1 there are many ways to produce nanometric tin oxide powders. It is known that specific properties of materials, useful in catalysis, can be enhanced by reducing particle size to nanoscale dimensions. Following on our past work with organometallic precursors as source of nanoparticles, we have decided to investigate the photocatalytic properties of nanoparticles of SnO_2 on Al_2O_3 towards the degradation of Indigo Carmine.

3.1. Thermogravimetric experiments

A study of the thermal behaviour of the samples (**1**)–(**3**) revealed a complex pyrolysis profile, with combined mass losses from organotin fragments and $Al(OH)_3$. Two composites (**1**) and (**2**) lose weight up to 430 °C and (**3**) at 600 °C.

3.2. X-ray powder diffraction

The XRD results are displayed in Fig. 1. Samples (**1**)–(**3**) exhibited diffraction lines arising from SnO_2 in planes (1 1 0), (1 0 1), (2 0 0), (2 1 1), (2 2 0) and (3 1 0). Lines corresponding to Al_2O_3 were not detected due its low crystallinity. As the unit cell parameters calculated for the SnO_2 in the composites, using the *unit cell* program [44], are close to those for pure SnO_2 (a = 4.738 Å and c = 3.187 Å), it is clear that Sn^{4+} has not replaced Al^{3+} in the unit cell of Al_2O_3. If such had occurred, materials (**1**)–(**3**) would have adopted a pseudo tri-dimensional polymeric net with bridging –O–Al–O–Sn–O–Al–O– units. Thus it appears that SnO_2 and Al_2O_3 segregate during the decomposition process leading to separate phases in the composites.

The (1 1 0) diffraction line was used to estimate the average crystallite sizes of SnO_2 (D), calculated from the (1 1 0) diffraction line using the Scherrer equation [45] were $D_{(\mathbf{1})}$ = 36 nm, $D_{(\mathbf{2})}$ = 22 nm and $D_{(\mathbf{3})}$ = 31 nm.

3.3. ^{119}Sn Mössbauer spectroscopy

The ^{119}Sn Mössbauer parameters, isomer shift (δ) and quadrupole splitting (Δ), were obtained. The isomer shifts for the composites, 0.01, 0.01 and 0.02 mm s^{-1}, for (**1**), (**2**) and (**3**), respectively, are somewhat smaller than the value for pure SnO_2 (0.03 mm s^{-1}) suggesting a small variation in the SnO_2 environment, however the presence of one Sn(IV) site in each sample [46] is clear. The isomer shift parameters are very different from the known values for $[SnBuO_{1.5}]_4$ or $SnBuCl_3$ [44], indicating complete pyrolysis into tin(IV) inorganic materials.

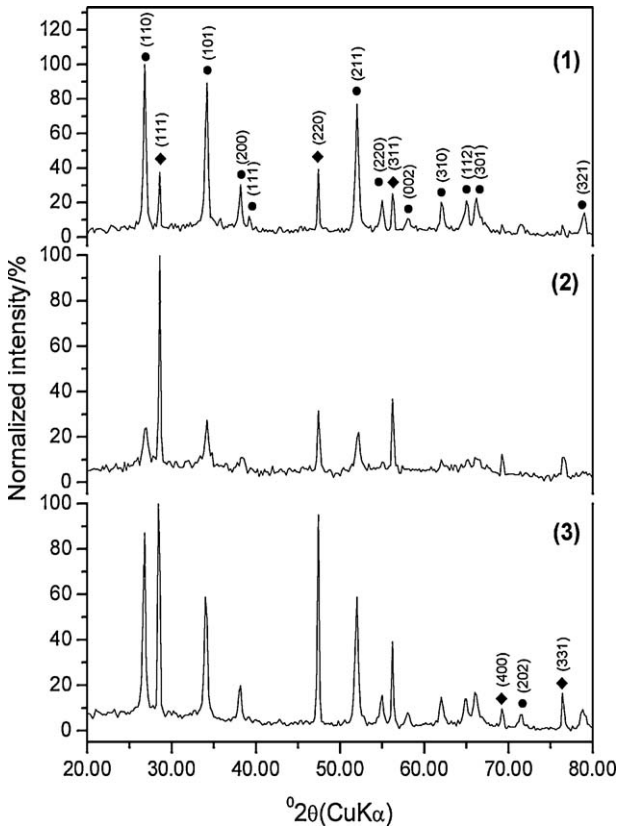

Fig. 1. X-ray powder diffraction patterns of the composites (**1**)–(**3**) (●, SnO_2; ◆, Si, internal standard).

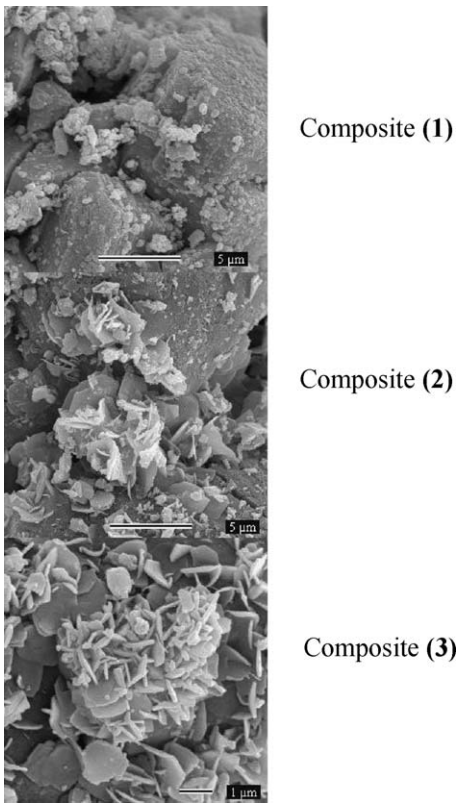

Fig. 2. The scanning electron microscopy (SEM) image of the composites (**1**)–(**3**).

The non-zero quadrupole splitting (Δ) 0.61 mm s^{-1} (**1**), 0.64 mm s^{-1} (**2**), 0.64 mm s^{-1} (**3**), showed a break of symmetry at the Sn center, possibly by the existence of oxygen vacancies accounting for the deviation in the δ parameters. The ^{119}Sn Mössbauer data validate the XRD results, reinforcing the conclusion that no polymeric –O–Al–O–Sn–O–Al–O– structural scheme is present in the materials.

3.4. X-ray electron probe microanalyses (EPMA)

The EPMA analysis revealed that oxygen, aluminium and tin are present in all samples. The carbon detected in the analysis came from the procedure used to recover the samples and is not derived from non-decomposed organic fragments in the composites.

3.5. Scanning electron micrographs (SEM)

The SEM images of samples (**1**)–(**3**) (Fig. 2) reveal the presence of SnO_2 crystals on the surface of Al_2O_3. The small crystals of SnO_2 are more abundant as the concentration of Sn in the sample increases.

3.6. Photocatalytic degradation of Indigo Carmine performed by composites (1)–(3)

Blank experiments showed that an aqueous solution of Indigo Carmine (**4**) at pH 5 submitted to the UV irradiation presented no apparent changes. In the presence of composites (**1**)–(**3**), or SnO_2, but with no UV irradiation, these solutions also stayed unaltered. When exposed to the UV irradiation, however, the solutions containing the materials (**1**, **2**, **3**, SnO_2) underwent remarkable discoloration. The discoloration rate was monitored by UV/vis spectroscopy, measuring the decline in the absorbance at 610 nm (the dye λ_{max}) as a function of reaction time (Fig. 3). Hence, whereas the solution containing composite (**3**) was completely discolored after 40 min, composites (**1**) and (**2**), as well as SnO_2, caused a complete color removal after longer reaction times. These results thus suggest that material (**3**) was the most efficient in promoting the dye photodegradation.

Fig. 4 shows the absorption spectra (absorbance *versus* wavelength in the range of 200–1000 nm) of the primary solution of Indigo Carmine (at 30 μmol L^{-1}) as well as of aliquots, submitted to UV irradiation in the presence of composite (**3**), collected at assorted reaction times. The band centered at 610 nm loses intensity as the degradation proceeds, and after 40 min it finally disappears. The absorbance at two other wavelengths in the

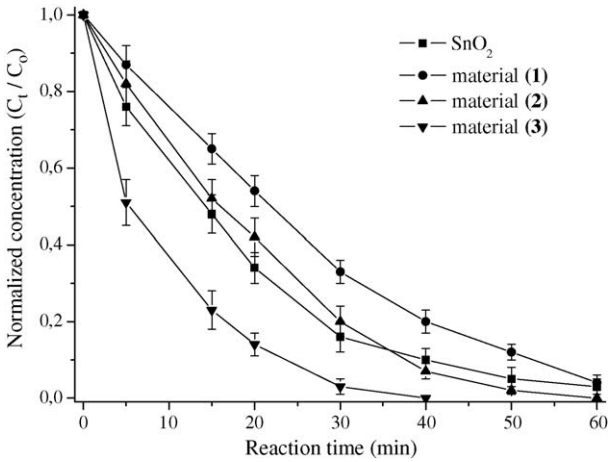

Fig. 3. Normalized Indigo Carmine concentration (C_t/C_o) as a function of reaction time.

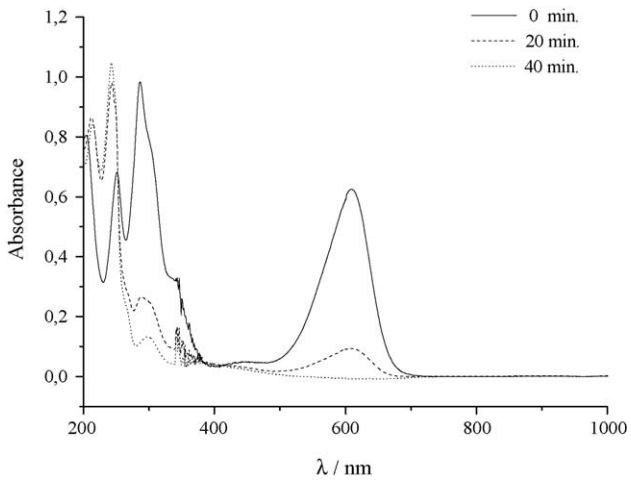

Fig. 4. UV–vis spectra of the initial aqueous solution of Indigo Carmine (at 30 μmol L^{-1}) and of the aliquots withdrawn after different times of exposition to the (**3**)/UV system.

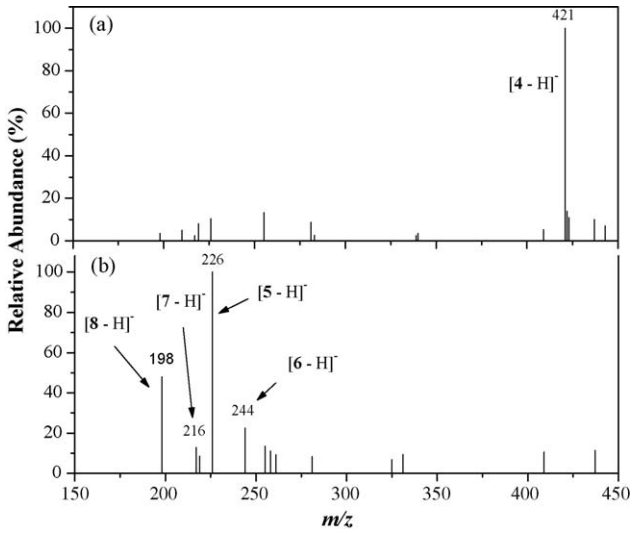

Fig. 5. (a) ESI(−)-MS of the initial aqueous solution of Indigo Carmine (**4**) at 30 μmol L^{-1}. (b) ESI(−)-MS of an reaction aliquot withdrawn after an exposition time of 40 min to the (**3**)/UV system.

UV region, 300 and 250 nm observed in the spectrum of Indigo Carmine, continuously shifts to lower wavelengths with reaction time: final values being near 230 and 210 nm, respectively. This is consistent with the degradation of Indigo Carmine leading to other aromatic products.

Electrospray ionization (ESI) is well-recognized to have a remarkable capability to gently transfer ionic species from the condensed to the gas phase, usually with no substantial in-source fragmentation [47]. Most importantly, it has been verified that the composition of the ESI-generated ions are closely related to that of solution [48]. In particular, electrospray ionization mass spectrometry (ESI-MS) is a very useful probe for the direct monitoring of reactions in aqueous solution [49–52]. The degradation of Indigo Carmine (**4**) in aqueous solution by composite (**3**) and UV irradiation was also investigated by using direct infusion ESI-MS. The ESI mass spectrum in the negative ion mode, ESI(−)-MS, of the initial Indigo Carmine aqueous solution and of the aliquot collected after a 40 min reaction time, is shown in Fig. 5a and b, respectively. The major anion, *m*/*z* 421, due to [**4**–H]$^-$, apparent in the mass spectrum of the initial dye solution (Fig. 5a), is no longer detected in the mass spectrum of the aliquot (Fig. 5b). The presence of other anions in this mass spectrum, of *m*/*z* 216, 226 and 244, indicated the formation of degradation products. Based on the *m*/*z* values of these anions, as well as on their fragmentation profiles (which show the formation of product ions arising from the release of small molecules as CO, CO_2, and H_2O, see Table 1), chemical structures for these products, as well as a route for the degradation of Indigo Carmine promoted by the **3**/UV system, could thus be proposed (Scheme 1).

Table 1
Main product ions arising from the mass-selection and dissociation of the anions [**5**–H]$^-$, [**6**–H]$^-$, and [**7**–H]$^-$.

Precursor ion (*m*/*z*)	Product ions (*m*/*z*; relative abundance, %)
[**5**–H]$^-$ (226)	[**5**–H–CO]$^-$ (198; 80)
[**6**–H]$^-$ (244)	[**6**–H–CO_2]$^-$ (200; 50)
	[**6**–H–CO_2–CO]$^-$ (172; 10)
[**7**–H]$^-$ (216)	[**7**–H–H_2O]$^-$ (198; 50)
	[**7**–H–CO_2]$^-$ (172; 60)

Hence, product (**5**), with a nominal mass of 227 Da and detected in its deprotonated form [**5**–H]$^-$ of *m*/*z* 226 (Fig. 5b), was

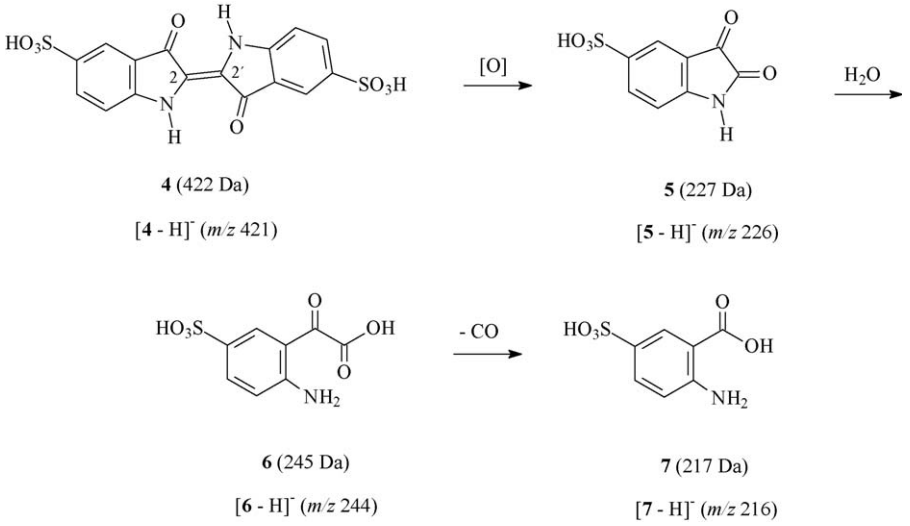

Scheme 1. Proposed reaction pathway for the degradation of Indigo Carmine (**4**) by the (**3**)/UV system in aqueous solution. Ions quoted under the structures are those detected by ESI(−)-MS.

postulated to be formed via an oxidative cleavage of the dye (**4**), as displayed in Scheme 1. Since (**5**) has no extensive electronic conjugate system as does (**4**), it will be silent in the visible region of the absorption spectrum. The formation of the other products (**6**) and (**7**) detected as the $[M-H]^-$ anions (m/z 244 and 226, respectively), then follows from (**5**). It is important to mention that in a previous work, our group performed the monitoring of the ozonation of Indigo Carmine in aqueous medium by direct infusion ESI-MS. The results also revealed the formation of the same sort of products, i.e. (**5**), (**6**), and (**7**) [52].

4. Summary of the results

Organotin halide $SnBuCl_3$ was reacted at different mole ratios with $Al(OH)_3$ and NH_4OH in ethanol. Thermolysis of the $SnBuCl_3$/$Al(OH)_3$ species at different temperatures produced composites containing molar ratios of Sn/Al_2O_3 of 30%, 40%, and 60% by weight. XRD results demonstrated the presence of nanometric SnO_2 particles in the composites, while SEM images indicated the presence of the SnO_2 crystals on the surface of Al_2O_3. These composites exhibited satisfactory photocatalytic activity in the degradation of the dye Indigo Carmine in aqueous medium. The experiments revealed that composite (**3**) effects better photocatalytic activity than (**1**), (**2**), and pure SnO_2. Electrospray ionization mass spectrometry and tandem mass spectrometry (ESI-MS and MS–MS) were used to elucidate the degradation pathway of this pollutant by composite (**3**) in the presence of UV irradiation.

Acknowledgements

We thank CNPq and FAPEMIG for financial support.

References

[1] S.R. Wang, J. Huang, Y.Q. Zhao, S.P. Wang, X.Y. Wang, T.Y. Zhang, S.H. Wu, S.M. Zhang, W.P. Huang, J. Mol. Catal. A: Chem. 259 (2006) 245.
[2] G.M. Maksimov, M.A. Fedotov, S.V. Bogdanov, G.S. Litvak, A.V. Golovin, V.A. Likholobo, J. Mol. Catal. A: Chem. 158 (2000) 435.
[3] D.E. Williams, K.F.E. Pratt, J. Chem. Soc. Faraday 94 (1998) 3493;
J.Y. Wei, Y.X. Zhu, Y.C. Xie, Chin. J. Catal. 24 (2003) 137.
[4] W. Gopel, K.D. Schierbaum, Sens. Actuators B 1 (1995) 26.
[5] J.C. Alonso, M. Garcia, A. Ortiz, J. Toriz, Semicond. Sci. Technol. 11 (1996) 243.
[6] L.S. Price, I.P. Parkin, A.M.E. Hardy, R.J.H. Clark, T.G. Hibbert, K.C. Malloy, Chem. Mater. 11 (1999) 1792.
[7] S.H. Park, V.C. Son, W.S. Willis, S.L. Suib, K.E. Creasy, Chem. Mater. 10 (1998) 2389.
[8] Z. Zainal, M.Z. Hussein, A. Kassim, A. Ghazali, J. Mater. Sci. Lett. 16 (1997) 1446.
[9] B. Subramanian, T. Mahalingan, C. Sanjeeviraja, M. Jayachandran, M.J. Chockalingan, Bull. Electrochem. 14 (1998) 398.
[10] D. Barreca, S. Garon, P. Zanella, E. Tondello, J. Phys. IV 9 (1999) 667.
[11] E. Shauti, A. Banerjee, V. Dutta, K.L. Chopra, J. Appl. Phys. 53 (1982) 1615.
[12] A.L. Dawar, J.C. Joshi, J. Mater. Sci. 19 (1984) 1.
[13] H. Hiramatsu, W.S. Seo, K. Koumoto, Chem. Mater. 10 (1998) 3033.
[14] R.J. Francis, S.J. Price, J.S.O. Evans, S. O'Brien, D. O'Hare, S.M. Clark, Chem. Mater. 8 (1996) 2102.
[15] G.A. Shaw, I.P. Parkin, Main Group Met. Chem. 19 (1996) 499.
[16] C.Y. Tan, Y.Y. Xia, Y.P. Chen, S.Y. Li, J.T. Liu, X.D. Liu, B.Z. Xu, J.H. Li, W.J. Cao, J. Appl. Phys. 73 (1993) 4266.
[17] P. Balaz, T. Ohtani, Z. Bastl, E. Boldizanova, J. Solid State Chem. 144 (1999) 1.
[18] R. Larciprete, E. Borsella, P. De Padova, P. Perfetti, C. Crotti, J. Vac. Sci. Technol. A 15 (1997) 2492.
[19] A.M.B. van Mol, Y. Chae, A.H. McDaniel, M.D. Allendorf, Thin Solid Films 502 (2006) 72.
[20] A.G. Pereira, A.O. Porto, G.G. Silva, G.M. de Lima, H.G.L. Siebald, J.L. Neto, Phys. Chem. Chem. Phys. 4 (2002) 4528.
[21] A.G. Pereira, L.A.R. Batalha, A.O. Porto, G.M. de Lima, G.G. Silva, J.D. Ardisson, H.G.L. Siebald, Mater. Res. Bull. 38 (2003) 1805.
[22] G.M. de Lima, A.O. Porto, J.D. Ardisson, A.C. Doriguetto, J. Ellena, C.L. Donnici, D.C. Menezes, Polyhedron 23 (2004) 2103.
[23] A.O. Porto, G.M. de Lima, A.G. Pereira, L.A.R. Batalha, J.D. Ardisson, Appl. Organomet. Chem. 18 (2004) 39.
[24] A.G. Pereira, A.O. Porto, G.M. de Lima, H.G.L. Siebald, J.D. Ardisson, Solid State Commun. 127 (2003) 223.
[25] A.C.B. Silva, A.F. Mesquita, E. de Moura Neto, A.O. Porto, G.M. de Lima, J.D. Ardisson, F.S. Lameiras, Solid State Commun. 135 (2005) 677.
[26] A.C.B. Silva, A.F. Mesquita, E. de Moura Neto, A.O. Porto, G.M. de Lima, J.D. Ardisson, F.S. Lameiras, Mater. Res. Bull. 40 (2005) 1497.
[27] A.C. Bose, P. Thangadurai, S. Rmasamy, V. Ganesan, S. Asokan, Nanotechnology 17 (2006) 1752;
S.A. Papargyri, D.N. Tsipas, D.A. Papargyris, A.I. Botis, A.D. Papargyris, Solid State Phenom. 106 (2005) 57;
J. Tamaki, Sens. Lett. 3 (2005) 89.
[28] H. Teteycz, R. Klimkiewicz, M. Maniecki, Appl. Catal. A: Gen. 274 (2004) 49.
[29] Z.Q. Liu, J. Ma, X.Y. Yang, Chin. J. Catal. 25 (2004) 624.
[30] R. Hertzenberg, Ver. Miner. 4 (1932) 33;
R. Kneip, D. Mootz, U. Severin, H. Wunderlich, Acta Crystallogr. Sect. B 38 (1982) 2022.
[31] C.L. Bowes, S. Petrov, G. Vovk, D. Young, G.A. Ozin, R.L. Bedard, J. Mater. Chem. 8 (1998) 711.
[32] N.L.V. Carreno, A.P. Maciel, E.R. Leite, P.N. Lisboa, E. Longo, A. Valentini, L.F.D. Probst, C.O. Paiva-Santos, W.H. Schreiner, Sens. Actuators B: Chem. 86 (2002) 185.
[33] F.R. Tabreu, M.B. Alves, C.C.S. Macedo, L.F. Zara, P.A.Z. Suarez, J. Mol. Catal. A: Chem. 227 (2005) 263.
[34] H. Lin-Rui, Y. Chang-Zhou, Y. Peng, J. Hazard. Mater. B139 (2007) 310.
[35] G. Crini, P.M. Badot, Prog. Polym. Sci. 33 (2008) 399.
[36] T. Robinson, G. McMullan, R. Marchant, P. Nigam, Bioresour. Technol. 77 (2001) 247.
[37] I.M. Banat, P. Nigam, D. Singh, R. Marchant, Bioresour. Technol. 58 (1996) 217.
[38] Z. Zainal, L.K. Hui, M.Z. Hussein, Y.H. Taufiq-Yap, A.H. Abdullah, I. Ramli, J. Hazard. Mater. 125 (2005) 113.
[39] C. Hachem, F. Bocquillon, O. Zahraa, M. Bouchy, Dyes Pigments 49 (2001) 117.
[40] A.P.F.M. de Urzedo, C.C. Nascentes, M.E.R. Diniz, R.R. Catharino, M.N. Eberlin, R. Augusti, Rapid Commun. Mass Spectrom. 21 (2007) 1893.
[41] JCPDS—Joint Committee on Powder Diffraction Standards, Mineral Powder Diffraction Files Data Book, International Center for Diffraction Data, Swarthmore, PA, 1997.
[42] T.J.B. Holland, S.A. Redfern, Miner. Mag. 61 (1997) 65.
[43] B.D. Culity, Elements of X-ray Diffraction, Addison-Wesley, London, 1978.
[44] P.J. Smith, Organomet. Chem. Rev. A 5 (1970) 373.
[45] J.B. Fenn, M. Mann, C.K. Meng, S.F. Wong, C.M. Whitehouse, Mass Spectrom. Rev. 9 (1) (1990) 37;
S.J. Gaskell, J. Mass Spectrom. 32 (1997) 677.
[46] P. Chen, Angew. Chem. Int. Ed. 42 (2003) 2832;
C. Hinderling, C. Adlhart, P. Chen, Angew. Chem. Int. Ed. 37 (1998) 2685;
R.M.S. Pereira, V.I. Paula, R. Buffon, D.M. Tomazela, M.N. Eberlin, Inorg. Chim. Acta 357 (2004) 2100.
[47] I. Dalmazio, M.O. Almeida, R. Augusti, T.M.A. Alves, J. Am. Soc. Mass Spectrom. 18 (2007) 679.
[48] I. Dalmazio, L.S. Santos, R.P. Lopes, M.N. Eberlin, R. Augusti, Environ. Sci. Technol. 39 (2005) 5982.
[49] M.H. Florencio, E. Pires, A.L. Castro, M.R. Nunes, C. Borges, F.M. Costa, Chemosphere 55 (2004) 345.
[50] P. Madeira, M.R. Nunes, C. Borges, F.M.A. Costa, M.H. Florencio, Rapid Commun. Mass Spectrom. 19 (2005) 2015.
[51] L.S. Santos, L. Knaack, J.O. Metzger, Int. J. Mass Spectrom. 246 (2005) 84.
[52] I. Dalmazio, A.P.F.M. de Urzedo, T.M.A. Alves, R.R. Catharino, M.N. Eberlin, C.C. Nascentes, R. Augusti, J. Mass Spectrom. 42 (2007) 1273.